

Platinum- and palladium-containing carbon nanomaterials as catalysts for hydrogenation and hydrogenating amination

N. A. Magdalinova,^{a*} M. V. Klyuev,^a T. G. Volkova,^a N. N. Vershinin,^b V. A. Bakaev,^b O. N. Efimov,^b and I. I. Korobov^b

^aIvanovo State University,

39 ul. Ermaka, 153025 Ivanovo, Russian Federation.

Fax: +7 (493 2) 32 4677. E-mail: mn2408@mail.ru, klyuev@inbox.ru

^bInstitute of Problems of Chemical Physics, Russian Academy of Sciences,

1 prosp. Akad. Semenova, Moscow Region, 142432 Chernogolovka, Russian Federation.

Fax: +7 (496) 517 8910. E-mail: vernik@icp.ac.ru

The catalytic activity of the carbon nanomaterials containing platinum and palladium in the model reactions of liquid-phase hydrogenation of nitrobenzene and hydrogenating amination was investigated. The catalytic systems based on nanodiamonds are more efficient than platinum-containing fullerene black, multi-walled nanotubes, and carbon nanofibers.

Key words: carbon nanomaterials, Pt and Pd catalysts, hydrogenation of nitrobenzene, hydrogenating amination, catalytic activity.

Presently, studies of the synthesis of efficient catalysts based on carbon nanomaterials (CNM) for many practical applications are carried out in many countries. In order to prepare catalytic systems with the highly developed catalytically active surface, it is necessary to obtain nano-sized particles with an optimum porous structure. Therefore, the use of CNM as supports for Platinum Group metals seems promising for the development of new catalytically active materials and catalytic systems. The catalytically active carbon nanomaterials containing platinum and palladium clusters with the crystallites in the 1 to 1.2 nm range were produced over the past several years.^{1–18} We have shown^{19,20} for the first time that the use of detonation nanodiamonds (ND) as supports for the Platinum Group metal makes it possible to obtain platinum clusters with the characteristic dimensions: 5 nm in diameter and the thickness from 0.4 to 1.2 nm. Such catalysts can find use in systems of air purification from carbon monoxide.²⁰

In this work, we consider the possibility to use the CNM-based catalysts in liquid-phase reactions of hydrogenation and hydrogenating amination. These reactions play an important in pharmaceutical industry to manufacture drugs of new generations using economical ecologically safe wasteless technologies.

Experimental

Synthesis of metal-containing carbon nanomaterials. For the anchoring of Pt clusters, a suspension of multi-walled nanotubes was preliminarily subjected to sonication-assisted in an H₂SO₄–HNO₃ mixture at 40 °C for 4 h. Nanofibers were oxidized on prolong (24 h) heating in concentrated nitric acid at

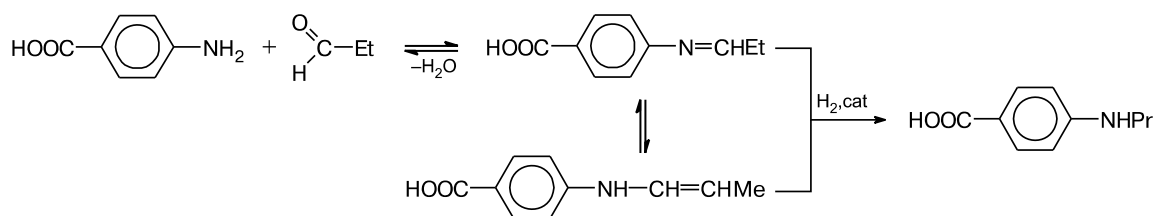
70 °C. The oxidized CNM were filtered off, washed with bidistilled water to the neutral pH, and dried in air. Fullerene black (FB) was used without preliminary preparation. The suspensions of the oxidized CNM (the concentration of the CNM was ≤ 5 g L^{–1}) for 20 min were treated by sonication. Then a solution of H₂PtCl₆·xH₂O (the platinum concentration was lower than 4 g L^{–1}) was added to the CNM suspension with continuous stirring in the presence of pyridine (0.5 mL) for 2–3 h, and the mixture was refluxed for 0.5–1 h. For platinum reduction, formic acid (10 mL) and a solution of sodium carbonate (~10 g in 50 mL of water) were added to the reaction mixture. The mixture was stored for 12 h, and the precipitate was filtered off, washed with water to the neutral pH, and dried in air. The commercial catalyst Pt/C 20% E-TEK was used for comparison.

Nanodiamonds containing Pd or Pt were synthesized according to the patented method.² Detonation ND with the specific surface 307–314 m² g^{–1} (the average size of the crystalline diamond core of the ND particles was ~4 nm) and the total content of non-carbon admixtures ≤ 0.5 wt.%. The samples of the Pd- and Pt-containing ND were mixed with active carbon in a weight ratio of 18 : 82 (the total weight was 1 g).

The average sizes of metal crystallites were calculated using the Sherrer equation from the powder diffraction patterns of the samples (ThermoARL diffractometer, Cu-Kα radiation, λ = 1.5406 Å).

The composition of samples Pt/ND and Pd/ND was determined by electron probe X-ray microanalysis, and the specific surface was determined by the BET method. Electron probe X-ray microanalysis was carried out on a VEGA TS 5130MM fully PC-controlled scanning electron microscope (CamScan MV2300)TP1PT) equipped with secondary electron (SE) and backscatter electron (BSE) detectors of YAG-crystals and an energy dispersive X-ray (EDX) microanalyzer with an INCA Energy2 semiconducting Si(Li) detector. The electron probe X-ray microanalysis results were calculated using the INCA En-

Scheme 1



ergy 200 program followed by the recalculation of the obtained data by the TP3PT program package developed at the Institute of Experimental Mineralogy, Russian Academy of Sciences. The studies were carried out at an accelerating voltage of 20 kV. The absorbed electron current on the standard cobalt sample was 516–565 pA and that on the studied sample was 540–620 pA. The size of the electron probe on the sample surface was 157–200 nm. Admixtures of titanium were ≤ 0.3 wt.%, and those of chlorine were $\leq 0.1\%$. The sol content of the initial nano-diamond was ≤ 2 wt.%.

Procedure of studying the reactions of hydrogenation of nitrobenzene and hydrogenating amination of propanal with 4-aminobenzoic acid. Experiments for the hydrogenation of nitrobenzene were performed with the catalyst (30 g) and NaBH_4 (10 mg) were placed in the reactor under the solvent (10 mL of ethanol) layer and activated for 10 min. Nitrobenzene (1 mmol) was introduced in a flowing hydrogen ($T = 318$ K, $P_{\text{H}_2} = 0.1$ MPa). After hydrogenation of one nitrobenzene portion conducted in the presence of Pt/ND and Pd/ND, another portion was introduced and the hydrogenation was carried out. All in all five portions of nitrobenzene were used.

Experiments for the hydrogenating amination of propanal with 4-aminobenzoic acid (Scheme 1) were performed with the catalyst (30 mg) and NaBH_4 (10 mg) placed in the reactor under the solvent layer (5 mL) and activated for 10 min. Then 4-aminobenzoic acid (2 mmol, 0.274 g) and propanal (2 mmol, 0.15 mL) dissolved in ethanol (20 mL) were introduced, the reactor was swept with hydrogen, and the process was carried out under the same conditions. Under the studied conditions, the reactions were zero order to the substrate and first order to the catalyst and hydrogen.

The apparent reaction rate constant was measured using the volumetric method from hydrogen absorption measurements. For comparison of the catalytic activity of the studied objects, we used the turnover number of the catalyst ($\text{TON}/\text{mol g-at.}^{-1} \text{ min}^{-1}$), which shows the number of moles of the substrates transformed per 1 g-at. of metal per 1 min

$$\text{TON} = W/(V_{\text{mol}}M),$$

where W is the hydrogen consumption rate, mL min^{-1} ; V_{mol} is the molar volume, mL mol^{-1} ; and M is the amount of the metal, g-at.

The hydrogenation products were analyzed using a chromatograph with a flame-ionization detector and a chromatographic glass column (diameter 3 mm, length 2000 mm) packed with Lucopren G-1000 (5%) on Chromaton N-AW-DMCS with argon as a carrier gas (the evaporation temperature was 200 °C, the temperature of the column was 230 °C, the carrier gas flow

rate was $1.60 \pm 0.02 \text{ L h}^{-1}$, and the volume of the introduced sample was 0.1–0.5 μL).

Results and Discussion

The specific surface area of the obtained samples of the platinum- and palladium-containing CNM varies from 22 to 295 $\text{m}^2 \text{g}^{-1}$. The metal clusters of the catalyst supported on ND have higher specific surface area than other metal–carbon catalysts. When the metal is dispersed on fullerene black and ND, the average size of Pt and Pd particles is 4–5 nm. For Pt supporting on carbon nanofibers (Pt/NF) and multi-walled carbon nanotubes (Pt/MNT), the average metal particle size is independent of the nature of CNM and the amount of supported Pt, being 6–8 nm (Table 1). If the metal is supported on carbon fibers 100–200 nm in diameter, the surface area of the catalyst decreases slightly as the metal concentration increases from 5 to 24.1 wt.% (see Table 1, entries 6 and 7). However, in an analogous experiment with CNM, no reduction of the surface is observed (see Table 1, entries 3 and 4). The fivefold increase in the diameter of the carbon nanofibers increases the surface area of the catalyst by a factor of two (see Table 1, entries 5 and 7).

It follows from the experimental data that the nature of CNM depends on the catalyst surface area rather than on the particle size of the supported metal. Since the size of metallic crystallites does not increase with an increase in the total metal content in the CNM, it can be assumed that a considerable number of free functional groups capable of participating in catalysis, for example, favoring the orientation of substrate molecules, remain on the CNM surface.

An analysis of the obtained experimental data (see Table 1) showed that all studied platinum- and palladium-containing CNM exhibit catalytic activity in the both model reactions. Under the same conditions, the rate of aniline formation in the reaction of nitrobenzene (NB) hydrogenation is substantially higher than the rate of formation of secondary amine (4-(propylamino)benzoic acid) in the reaction of hydrogenating amination of propanal with 4-aminobenzoic acid (PABA) (see Table 1). This regularity can be explained by either different mechanisms of hydrogenation of the nitro group and $>\text{C}=\text{N}-$ bond, or

Table 1. Characteristics of the catalysts and the rates of amine formation in the reactions of hydrogenation and hydrogenating amination

Entry	Catalyst	d^a/nm	$S^b/\text{m}^2 \text{ g}^{-1}$	$W_{\text{an}} \cdot 10^4$	$W_{\text{sec}} \cdot 10^6$
				$\text{mol L}^{-1} \text{ s}^{-1}$	
1	Pt(20%)/C (E-TEK)	2.5	181	3.80	37.5
2	Pt(10%)/FB	4–5	280	—	16.0
3	Pt(4.4%)/MNT	6–8	22	1.10	7.5
4	Pt(22.6%)/MNT	6–8	24	1.90	24.8
5	Pt(26.6%)/NF ($d = 20\text{--}40 \text{ nm}$)	6–8	42	2.00	16.3
6	Pt(5%)/NF ($d = 100\text{--}200 \text{ nm}$)	6–8	116	—	10.4
7	Pt(24.1%)/NF ($d = 100\text{--}200 \text{ nm}$)	6–8	97	3.20	22.6
8	Pt(15%)/ND	5.0	295	3.09	4.7
9	Pt(20%)/ND	5.0	288	2.97	9.1
10	Pt(25%)/ND	5.0	277	2.96	18.0
11	Pd(6%)/ND	5.0	284	2.82	11.0
12	Pd(10%)/ND	5.0	267	5.16	18.0
13	Pd(15%)/ND	5.0	263	7.96	17.0

^a Average size of the metal particles.^b Specific surface area of the catalyst surface.

by spatial factors: the nitro group is more accessible to activated hydrogen than the $>\text{C}=\text{N}-$ bond screened from two sides.

The maximum rate for aniline formation (W_{an}) is characteristic of the catalysts Pd(10%)/ND and Pd(15%)/ND (see Table 1, entries 12 and 13). In hydrogenating amination, the highest rate for secondary amine formation is observed for the catalyst Pt/C (trade mark E-TEK, see Table 1).²¹ The fivefold increase in the content of Pt supported on the MNT results only in a threefold increase in the rate of formation of 4-(propylamino)benzoic acid (W_{sec}) and less than twofold increase in the rate for aniline formation (see Table 1, entries 3 and 4). For Pt supporting on the carbon nanofibers 100–200 nm in diameter, it was found that as the metal content increases nearly fivefold the formation of secondary amine increases by a factor of 2.2. For the catalyst Pt/NF with 26.6% Pt supported on the nanofibers with a diameter of 20–40 nm, the value of W_{sec} is 1.4 times lower than the rate obtained on the catalyst Pt(24.1%)/NF with a diameter of the nanofibers of 100–200 nm. In the presence of the ND-based catalysts, with the increasing metal content, a 1.5–1.8 time increase was observed for the rate of aniline formation in the case of Pd/ND (see Table 1, entries 11–13) and almost no change in the rate in the case of Pt/ND was observed (see Table 1, entries 8–10). The situation is opposite for hydrogenating amination: the rate for secondary amine formation for Pt/ND doubles with an increase in the supported metal content (see Table 1, entries 8–10), whereas no direct dependence is observed for Pd/ND (see Table 1, entries 11–13).

The values of the rate for aniline formation in the reaction of nitrobenzene hydrogenation for five successively

reduced portions are presented in Fig. 1. It is seen that for the hydrogenation of the second portion of nitrobenzene the value of W_{an} is slightly higher than that for the hydrogenation of the first portion, and then W_{an} remains unchanged upon the introduction of the next portion of nitrobenzene, indicating stability of catalytic performance of the studied samples.

Since the catalysts differ both in the metal content and the surface area, we compared the turnover numbers for the reaction (Table 2). It turned out that the activity of the Pt- and Pd-CNM catalysts in nitrobenzene hydrogenation is 4–25 times higher than in the hydrogenating amination of propanal with 4-aminobenzoic acid. Taking into

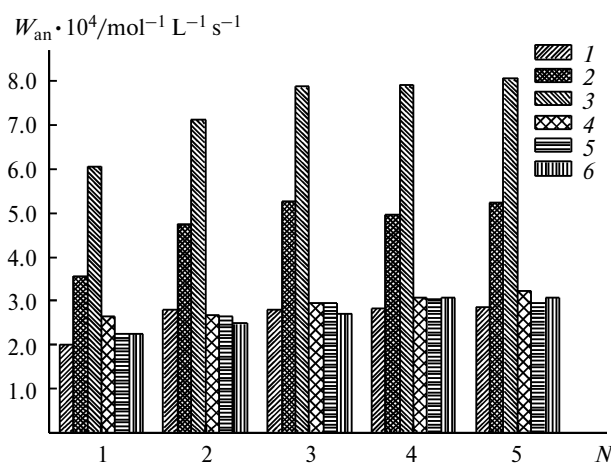


Fig. 1. Rate of aniline formation in nitrobenzene hydrogenation using various catalysts: Pd(6%)/ND (1), Pd(10%)/ND (2), Pd(15%)/ND (3), Pt(15%)/ND (4), Pt(20%)/ND (5), and Pt(25%)/ND (6); N is the number of portions of nitrobenzene.

Table 2. Efficiency of the Pt- and Pd-CNM* in the hydrogenation of nitrobenzene and the hydrogenating amination of propanal with 4-aminobenzoic acid

Entry	TON/mol g-at. ⁻¹ min ⁻¹		TON/S/mol g-at. ⁻¹ min ⁻¹ m ⁻²	
	NB	PABA	NB	PABA
1	11.2	1.8	2.1	0.3
2	—	1.6	—	0.2
3	14.6	1.7	22.1	2.6
4	4.9	1.1	6.8	1.5
5	4.5	0.6	3.6	0.5
6	—	2.0	—	0.6
7	7.7	0.9	2.6	0.3
8	42.2	1.7	26.5	1.1
9	32.2	2.5	20.7	1.6
10	25.7	3.9	17.2	2.6
11	55.5	5.4	36.2	3.5
12	59.9	5.2	41.5	3.6
13	65.0	3.3	45.5	2.3

* The characteristics of the CNM-based catalysts used in various experiments are given in Table 1.

account the surface area of the catalyst (see Table 2) does not change this trend.

Among the catalysts based on multi-walled nanotubes, the catalyst Pt(4.4%)/MNT has the highest efficiency of the use of platinum: it is almost 3 times more efficient than the catalyst Pt(22.6%)/MNT in nitrobenzene hydrogenation and 1.5 times more efficient than this catalyst in hydrogenating amination (see Table 2, entries 3 and 4). A comparison of the catalysts based on carbon nanofibers shows that a high efficiency is observed for Pt/NF with a diameter of nanofibers of 100–200 nm and a smaller weight content of platinum (see Table 2, *cf.* entries 5–7).

With an increase in the content of palladium supported on ND the activity of the catalysts increases in nitrobenzene hydrogenation and decreases in hydrogenating amination. The dependence is inverse for Pt/ND: with an increase in the platinum content the efficiency of the catalysts decreases for nitrobenzene hydrogenation and increases for hydrogenating amination. In this case, the hydrogenation and hydrogenating amination in the presence of Pd/ND are 1.4–2.6 and 1.3–2.3 times faster than those in the presence of Pt/ND.

As a whole, the catalysts based on ND are the most efficient among the samples studied (see Table 2). In terms of the efficiency in nitrobenzene hydrogenation, Pt/ND and Pd/ND are 8–22, 2.5–6.7, and 5–17.5 times superior to Pt/C (E-TEK), Pt/MNT, and Pt/NF, respectively. In the reaction of hydrogenating amination, Pt/ND and Pd/ND are 2–18 times more efficient than Pt/C (E-TEK), Pt/FB, and Pt/NF (see Table 2).

Thus, the catalytic liquid-phase hydrogenation of nitrobenzene and hydrogenating amination were carried out in the presence of the carbon nanomaterials with dif-

ferent weight contents of supported platinum and palladium. It was shown that the Pt- and Pd-ND in the studied reactions have higher catalytic activity and efficiency than other metal-containing CNM.

The authors are grateful to B. P. Tarasov (Institute of Problems of Chemical Physics, Russian Academy of Sciences) for kindly presented samples of platinum-containing nanomaterials based on multi-walled carbon nanotubes, nanofibers, and fullerene black.

This work was carried out in the framework of the program "Development of Basic Research in the Area of Creation of Functional Nanomaterials at the Educational Scientific Complex "Chemical Physics" of the Ivanovo State University and the Institute of Problems of Chemical Physics, Russian Academy of Sciences" (Project Nos 2.2.1.1.2820 and 2.2.1.1/11465).

References

1. P. Tribolet, L. Kiwi-Minsker, *Catal. Today*, 2005, **105**, 337.
2. C.-J. Su, L.-S. Hsu, T.-W. Wu, C.-J. Liu, S.-H. Lin, *Nanotech.*, 2003, **3**, 13.
3. C. Liang, W. Xia, H. Soltani-Ahmadi, O. Schlüter, R. A. Fischer, M. Muhler, *Chem. Commun.*, 2005, 282.
4. M. Takasaki, Y. Motoyama, K. Higashi, S. H. Yoon, I. Mochida, H. Nagashima, *Org. Lett.*, 2008, **10**, 1601.
5. Y. Zhao, Ch.-H. Li, Zh.-X. Yu, K.-F. Yao, Sh.-F. Ji, J. Liang, *Mat. Chem. Phys.*, 2007, **103**, 225.
6. W. Li, Ch. Liang, W. Zhou, J. Qiu, H. Li, G. Sun, Q. Xin, *Lett. Ed./Carbon*, 2004, **42**, 436.
7. H. Ma, L. Wang, L. Chen, C. Dong, W. Yu, T. Huang, Y. Qian, *Catal. Commun.*, 2007, **8**, 452.
8. C.-H. Li, Z.-X. Yu, K.-F. Yao, S.-F. Ji, J. Liang, *J. Mol. Catal. A: Chem.*, 2005, **226**, 101.

9. T. Onoe, Sh. Iwamoto, M. Inoue, *Catal. Commun.*, 2007, **8**, 701.
10. A. M. Zhang, J. L. Dong, Q. H. Xu, H. K. Rhee, X. L. Li, *Catal. Today*, 2004, **93–95**, 347.
11. V. Lordi, N. Yao, J. Wai, *Chem. Mater.*, 2001, **13**, 733.
12. T. Harada, S. Ikeda, M. Miyazaki, T. Sakata, H. Mori, M. Matsumura, *J. Mol. Catal. A: Chem.*, 2007, **268**, 59.
13. N. S. Kuyunko, S. D. Kushch, V. E. Muradyan, A. A. Volodin, V. I. Torbov, B. P. Tarasov, in *Hydrogen Materials Science and Chemistry of Carbon Nanomaterials*, Eds T. N. Veziroglu, S. Y. Zaginaichenko, D. V. Schur, B. Baranowski, A. P. Shpak, V. V. Skorokhod, A. Kale, NATO Security through Science, Series A, Chemistry and Biology, Springer Science—Business Media BV., 2006, 205.
14. S. D. Kushch, N. S. Kuyunko, B. P. Tarasov, in *Carbon Nanomaterials in Clean Energy Hydrogen Systems*, Eds B. Baranowski, S. Yu. Zaginaichenko, D. V. Schur, V. V. Skorokhod, A. Veziroglu, NATO Science for Peace and Security, Series-C: Environmental Security, Springer Science—Business Media B. V., Dordrecht, The Netherlands, 2008, 389.
15. S. D. Kushch, N. S. Kuyunko, B. P. Tarasov, *Zh. Obshch. Khim.*, 2009, **79**, 542 [*Russ. J. Gen. Chem. (Engl. Transl.)*, 2009, **79**, 706].
16. B. Coq, J. M. Planeix, V. Brotons, *Appl. Catal. A: General*, 1998, **173**, 175.
17. H. Vu, F. Gonçalves, R. Philippe, E. Lamouroux, M. Corrias, Y. Kihn, D. Plee, Ph. Kalck, Ph. Serp, *J. Catal.*, 2006, **240**, 18.
18. Z.-Z. Zhu, Zh. Wang, H.-L. Li, *J. Power Sources*, 2009, **186**, 339.
19. N. N. Vershinin, V. A. Bakaev, O. N. Efimov, I. I. Korobov, A. L. Gusev, A. A. Alexenskii, M. V. Baibakova, A. Ya. Vul', *Intern. Sci. J. Alternative Energy and Ecology*, 2009, 123.
20. N. N. Vershinin, V. A. Bakaev, A. L. Gusev, O. N. Efimov, *Inter. Sci. J. Alternative Energy and Ecology*, 2009, 67.
21. N. A. Magdalinova, M. V. Klyuev, T. G. Volkova, *Inter. Sci. J. Alternative Energy and Ecology*, 2009, 89.

Received March 4, 2011;
in revised form March 20, 2011